On the complexity of predicting tablet capping

J. Meynard [a], F. Amado-Becker [b], P. Tchoreloff [a], V. Mazel [a,*]

[a] Univ. Bordeaux, CNRS, Arts et Metiers Institute of Technology, Bordeaux INP, INRAE, I2M Bordeaux, F-33400 Talence, France
[b] Research and Development Division, F. Hoffmann-La Roche AG, Basel, Switzerland

A B S T R A C T

Predicting tablet defects, such as capping, that might occur during manufacturing, is a challenge in the pharmaceutical industry. In the literature, different parameters were presented to predict capping but no general consensus seems to have been reached yet. In this article, we chose to study a wide range of products (18 formulations, 8 of which presenting capping) to predict capping on biconvex tablets using the properties characterized on defect-free flat-faced tablets (tensile strength, solid fraction, elastic recovery, etc.), made using the same process parameters. Single parameters and predictive indices presented in the literature were evaluated on this set of formulations and were found not suitable to predict capping. A predictive model was then developed using a decision tree analysis and was found to depend only on three in-die tablet properties: the plastic energy per volume, the in-die elastic recovery and the residual die-wall pressure. This model was tested on another set of 13 formulations chosen to challenge it. The capping behavior of 29 out of the 31 formulations studied in total was well estimated using the developed model with only two products which were predicted to cap and did not. This shows the potential of the used approach in terms of risk analysis and assessment for capping occurrence.

1. Introduction

Capping is a common defect that can occur during the manufacturing of pharmaceutical tablets. It corresponds to a specific kind of failure pattern of the tablet, which is usually observed on tablets after ejection from the die. Considering biconvex tablets, a tablet is considered capped if one or both of cups come off of the tablet main body. It should not be confused with lamination, which is another kind of tablet defect, but with failure planes passing through the tablet band (Alderborn, 2001). Tablet failure occurs when the stress distribution in the tablet microstructure becomes higher than the material strength. In the case of capping for biconvex tablets, the contact loss between the tablet and the punches during the unloading phase leads to the appearance of a shear stress at the limit between the land and the cup (Hiestand et al., 1977; Mazel et al., 2015; Wu et al., 2008). For compacted granular materials such as tablets, their ability to resist to stresses relies on the quality of the bonds between the particles which constitute the material. When the shear stress distribution leads to the failure of the inter-particulate bond, the manufactured biconvex tablet loses its cohesion between the land and the cup, which leads to capping defects. Even if capping is known for more than a century (Wood, 1906), its mitigation can still be challenging today.

Being able to predict *a priori* the tendency of a formulation to cap when manufactured under specific conditions would be of great interest from an industrial perspective. As capping is related to the balance between the shear stress distribution and the tablet strength, it is logical to think that the parameters linked with these two aspects could be used as predictors of the capping tendency. Following this idea, in the literature, several authors suggested several critical parameters that could be linked with capping occurrence: high residual die wall pressures (Sugimori et al., 1989a), high tablet elastic recovery (Ritter and Sucker, 1980), high tablet anisotropy (Nyström et al., 1978), low tensile strengths (Wu et al., 2008)). (Hiestand et al., 1977) proposed the brittle fracture index (BFI), which is calculated by comparing the apparent tensile strength of tablets with a hole drilled in the middle to the tensile strength of tablets without holes, as an indicator of a material sensitivity to the presence of defects and stated that values equal or higher than 0.5 are related to tablets with a high tendency to cap or laminate (Okor et al., 1998). Other authors also proposed different kinds of more complex indices to predict capping (Akseli et al., 2013; Nakamura et al., 2012; Sugimori et al., 1989b). Compared to the previous studies, those indices are a combination of various material parameters and they try to express the influence, on the inter-particulate bonding, of different properties which can have counter-balancing effects. For example,

* Corresponding author at: Université de Bordeaux, CNRS, I2M Bordeaux, 146 rue Léo Saignat, F-33000 Bordeaux, France.
E-mail address: vincent.mazel@u-bordeaux.fr (V. Mazel).

(Nakamura et al., 2012) presented the hypothesis that the quality of tablet inter-particulate bonds is related to tablet ability to relieve stress through plastic and elastic deformations. Therefore, they suggested that high capping propensity occurs when the product of the tablet axial stress relaxation (property related to elastic deformations) and the plastic energy of the product (property related to plastic deformations) was low. (Krycer et al., 1982) proposed an indicator based on the gradient of the out-of-die height elastic recovery versus the residual die-wall pressure to evaluate the magnitudes of elastic and plastic deformations. (Sugimori et al., 1989b) proposed to predict capping by comparing the ratio of the maximum shear stress and strength. Another example is given by (Akseli et al., 2013)which proposed to express tablet capping tendency by comparing the tablet cohesion (using tablet tensile strength) to its ability to relieve stress through elastic and plastic deformations (using respectively the elastic recovery and the Heckel parameter). Note that, in the same article, (Akseli et al., 2013) also proposed to predict capping using anisotropic elastic ratios measured using the ultrasonic method. To do so, they manufactured biconvex tablets and evaluated the speed of sound in two perpendicular directions (normal and parallel to the compaction direction). Nevertheless, due to the convex tablet shape used, the tablet might present capping defects that might influence the wave speed. It is thus possible that the anisotropy found was in fact the consequence and not the cause of capping. It can thus not really be considered as a predictive index as the previous ones.

Despite this large literature on the subject, it seems that there is for the moment no consensus on which of these parameters or indices could be the more appropriate for capping prediction. It would thus be of interest to evaluate and compare their predictive capability. The goal of the present paper was to study how to predict *a priori* the capping behaviour of biconvex tablets with a given shape using characterizations performed on the same product but on flat-faced tablets presenting no defects. Of course it is well-known that capping is not only influenced by the powder properties but also by the process parameters (pressure, speed, etc.). In order not to mix these effects, we chose here to keep the manufacturing conditions (pressure, speed) constant to focus only on the influence of the properties of the formulation on capping when these manufacturing conditions are used.

To do so, a first wide set of formulations with different properties was characterized in order to evaluate the capping predictive capability of the parameters and indices presented in the literature. An approach using a machine learning tool was then performed on the database to identify key parameters for predicting capping. Finally, the accuracy of the predictive model obtained was evaluated and discussed on a second set of formulations.

2. Materials and methods

2.1. Materials

2.1.1. Raw materials

The idea of this study was to study products relevant for the pharmaceutical tableting and which presented a large diversity of behaviors. Therefore, the database developed included different types of products including excipients, disintegrants, binders, lubricants or active substances. The products used are the following:

- Alanine "Ala" (L-Alanine, Merck, Darmstadt, State of Hesse, Germany),
- Benzoic acid "ABenz" (Benzoic acid, Coopération Pharmaceutique Française, Melun, Ile-de-France),
- Microcrystalline cellulose "MCC" (Vivapur 12, JRS Pharma, Rosenberg, Bade-Wurtemberg, Germany),
- Crospovidone "Kol" (Kollidon CL, BASF, Ludwigshafen, Rhineland-Palatinate, Germany),
- Calcium sulfate dihydrate "CaSul" (Compactrol, JRS Pharma, Rosenberg, Bade-Wurtemberg, Germany),
- Dicalcium phosphate dihydrate "DCP" (Di-cafos D160, Chemische Fabrik Budenheim, Budenheim, Germany),
- Polyethylene glycol 5000 "PEG" (Polyox WSR N-80, Dow Chemical, Midland, Michigan, United States),
- Ibuprofen "Ibu" (Ibuprofen DC 85 W, BASF, Ludwigshafen, Rhineland-Palatinate, Germany),
- Granulated lactose "GLac" (SuperTab 30GR, DFE Pharma, Goch, Nordrhein-Westfalen, Germany),
- Spray dried lactose "SDLac" (SuperTab 14SD, DFE Pharma, Goch, Nordrhein-Westfalen, Germany),
- Coarse mannitol "CMan" (Mannitol, Coopération Pharmaceutique Française, Melun, Seine-et-Marne, France),
- Spray dried mannitol "SDMan" (Pearlitol 200SD, Roquette Frères, Lestrem, Pas-de-Calais, France),
- Pulverized paracetamol "Par" (Paracetamol powdered API, Caelo - Caesar & Loretz GmbH, Hilden, North Rhine-Westphalia, Germany),
- Anhydrous calcium phosphate "ACP" (Anhydrous Emcompress, JRS Pharma, Rosenberg, Germany),
- Anhydrous calcium phosphate "ACP60" (Di-cafos A60, Chemische Fabrik Budenheim, Budenheim, Germany),
- Tricalcium phosphate "TCP" (Tri-cafos 500, Chemische Fabrik Budenheim, Budenheim, Germany),
- Crosscaramellose sodium "CNa" (Vivasol, JRS Pharma, Rosenberg, Bade-Wurtemberg, Germany),
- Sorbitol "Sorb" (Neosorb XTab 300S, Frères, Lestrem, Pas-de-Calais, France),
- Directly compressible starch "DCSta" (StarTab, Colorcon, Barcelona, Spain),
- Partially pre-gelatinized starch "Sta" (Lycatab C, Roquette Frères, Lestrem, Pas-de-Calais, France),
- Magnesium stearate "MgSt" (Ligamed MF-2-V, Peter Greven, Bad Münstereifel, Nordrhein-Westfalen, Germany),
- Hypromellose acetate succinate "ASLMP" (AQOAT AS-LMP, Shin-Etsu, Chiyoda, Tokyo, Japan).

2.1.2. Blending process and pycnometric density determination

The raw products presented in the section above were used to obtain lubricated pure products (using MgSt as lubricant) and formulation-like mixtures. The composition of the mixtures used will be presented in section 1.3. In each case, mixtures of 200 g were weighed directly in a 1L recipient using a PB3002-S/PH balance (J.P., Mettler Toledo, Hospitalet De Llobregat, Catalonia, Spain). Blends were then performed using the T2F turbula mixer (Willy A. Bachofen, Muttenz, Switzerland) at 49 rpm. All the lubricated pure products were mixed together during 5 min. For the formulation-like mixtures, a first blend of 5 min was performed with the main ingredients (with composition in weight higher than 10%) then followed by a second blend of 5 min with the remaining raw materials (lubricants and disintegrants). Blends were stored under controlled atmosphere (20 °C and 44% RH) during at least 48 h before tablet manufacturing.

The apparent particle density ρ_{pyc} of each mixture was determined using a gaz pycnometer (Helium AccuPyc 1330, Micromeritics, Norcross, Georgia, USA) with helium. Each run (corresponding to 10 purges and 10 runs) was performed in a cell of 10 cm^3 with an equilibration rate of 0.05 psig/min and a pressure of 19.5 psig.

2.1.3. Tablet manufacturing

All the tablets were manufactured on a Styl'One Evolution compaction simulator (Medelpharm, Beynost, France). This device is a single station instrumented tableting machine equipped with strain gauge force sensors to measure the force on both punches. The displacement of each punch is monitored using incremental sensors. During the acquisition, the sampling rate was 5 kHz. The compaction cycle was set to simulate a Korsch XL 100 Euro-B at a rotation speed of

40 rpm. The dwell-time (time during which the punches remained stationary) was about 50 ms. Tablets were manufactured for each product at 200 MPa. For the purpose of the study, three pairs of Euro-B punches were used (as shown in Fig. 1): a) round concave punches with a diameter of $D = 11.28$ mm and a radius of curvature of R = 11 mm to obtain biconvex tablets (Fig. 1a), b) round flat punches with a diameter of D = 11.28 mm (Fig. 1b) and c) flat punches with a flattened disc geometry with a diameter of D = 11 mm and two parallel chords defined by a circular angle of $\alpha = 30^{\circ}$ (Fig. 1c). Both flat punches were used to obtain flat-faced cylindrical tablets: tablets with flattened ends will be referenced as FT tablets and those with a circular shape will be called CT tablets. Filling height was modified to obtain a final tablet height of 2 mm for flat-faced tablets and a final tablet band of 2 mm for biconvex tablets (BT). The compaction thickness was set to obtain the targeted axial pressure at the peak of compaction. An instrumented die using strain gauge technology was used to monitor the die-wall pressure for all the experiments except in the cases where the flattened disc geometry was used.

2.2. Methods

2.2.1. In-die measurements

Using the production reports of five CT tablets given by the compaction simulator, several in-die measurements were extracted for this study:

- The residual die-wall (radial) pressure $P_{rad,res}$, which corresponds to the die-wall pressure measured at the end of the unloading (when the axial pressure of the punches dropped to zero).
- The tablet plastic energy E_p (Alderborn, 2001), which is the plastic work dissipated by the granular medium during manufacturing. It is defined as the area between the compression and decompression curves on the curve axial force versus distance between the punches (which is related to the deformation of the medium during compaction). For better comparability between products with very different densities, the plastic energy of each formulation was normalized by the tablet solid volume (Wünsch et al., 2021). This normalized parameter will be referenced as $E_{p,v}$.
- The minimal height h_{min}, which corresponds to the minimal distance between the punches during compaction. This value takes into account the machine deformations during compaction.
- The in-die recovery height h_f, which is the distance between the punches at the end of the unloading step.

The in-die elastic recovery E_f (Hirschberg et al., 2020; Yohannes et al., 2015) was estimated as:

$$E_f = 100\left(\frac{h_f}{h_{min}} - 1\right)$$

Note that in-die tablet diameter remains constant thus the elastic recovery presented above characterized tablet dimension modifications in height as well as in volume.

The mean yield pressure P_y, which is defined as the reciprocal of the linear part of the Heckel plot (Heckel, 1961a, 1961b), was determined using the in-die curves of CT tablets. The regression on the linear region was performed based on the method of least squares ($R^2 > 0.99$).

To evaluate the stress relaxation of CT tablets, an axial stress relaxation parameter (Nakamura et al., 2012), referenced hereinafter as R_{40}, was estimated as:

$$R_{40} = 1 - \frac{P_{ax}\left(t = t_{comp} + 40\right)}{P_{ax}\left(t = t_{comp}\right)}$$

where $P_{ax}(t_{comp})$ and $P_{ax}(t = t_{comp} + 40)$ are the axial pressures when the maximum axial compaction pressure is reached (i.e. at t_{comp}) and 40 ms after t_{comp} respectively. Note that as the dwell-time was about 50 ms for the manufacturing cycle studied, only stress relaxation occurred during the period of time evaluated.

2.2.2. Out-of-die solid fraction and elastic recovery

Dimensions of five CT tablets were measured 48 h after being manufactured. Tablet solid fraction S_F was then estimated by the ratio between tablet density ρ_{tab} (evaluated with the measurements of tablet dimensions out of the die and mass) and pycnometric density ρ_{pyc}.

Using the dimensions of tablets out of the die, the height elastic recovery $E_{O,H}$ (Armstrong and Haines-Nutt, 1974; Krycer et al., 1982; Picker, 2001) and the volume elastic recovery $E_{O,V}$ (Haware et al., 2010; Maganti and Çelik, 1993; Mazel et al., 2013) were also estimated. $E_{O,H}$ was defined as:

$$E_{O,H} = 100\left(\frac{h_F}{h_{min}} - 1\right)$$

And $E_{O,V}$ was defined as:

$$E_{O,V} = 100\left(\frac{V_F}{V_{min}} - 1\right)$$

where h_F and V_F correspond to the height and volume measured out-of-the-die and V_{min} is the tablet volume when the minimal height h_{min} is reached.

2.2.3. Diametral compression

Diametral compression tests were performed on ten FT tablets using a TA.HDplus texture analyzer (Stable microsystems, United Kingdom). Compacts were compressed between two flat surfaces at a constant speed of 0.10 mm/s with an acquisition rate of 500 Hz. The breaking force F_r of each tablet was recorded. The tensile strength σ_T of each FT tablet was evaluated using the equation of (Mazel et al., 2016):

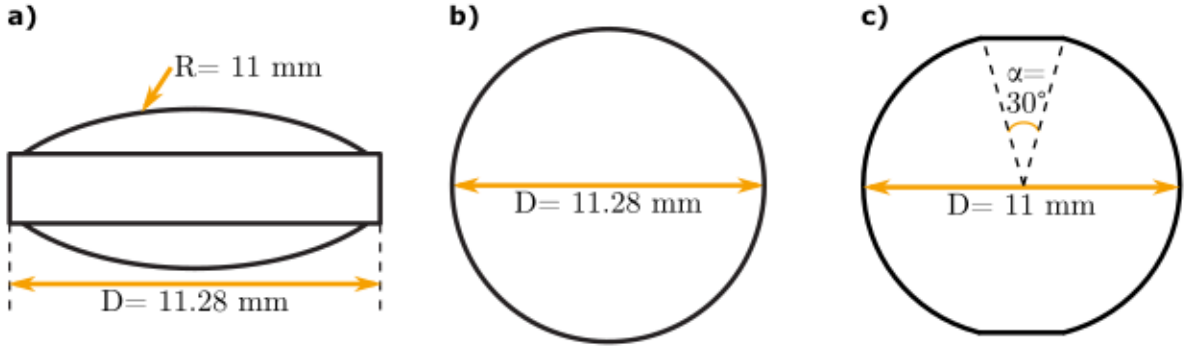

Fig. 1. Representation of the tablet geometries used in the study: a) side view of the biconvex tablets (BT), b) top view of the round flat tablets (CT) and c) top view of the flat tablet with flattened disc geometry (FT).

$$\sigma_T = 0.87\frac{2F_r}{\pi Dh} \quad (1)$$

where h and D are respectively the tablet height and diameter.

On five out of the ten tablets characterized with this test, holes of 1 mm of diameter were inserted on their center using a drill Micromot 50 E/EF (PROXXON S.A., Luxembourg). Machining speed was adapted for each formulation. The tablets were maintained using a specially designed polymeric holder obtained by 3D printing. To avoid defects at the back of the tablet during machining, two tablets were placed together and only the upper one was finally used for experiments. The brittle fracture index *BFI* introduced by (Hiestand et al., 1977) was thus characterized as:

$$BFI = \frac{1}{2}\left(\frac{[\sigma_T]_\emptyset}{[\sigma_T]_T} - 1\right)$$

where $[\sigma_T]_\emptyset$ and $[\sigma_T]_T$ were respectively the mean tensile strength obtained for the five tablets without holes and with the holes calculated with equation (1).

2.2.4. Impulse excitation

Impulse excitation tests were performed on five CT tablets following the methodology first presented in (Mazel and Tchoreloff, 2020). To induce sample vibrations, tablets were dropped on a hard surface (stainless steel), at a fixed height (1 cm height) to minimize the variation of energy given to the tablets during impact. In all the cases, to obtain a single rebound, tablets were dropped on their lateral band. Tablet free vibrations induced by impact were recorded using a microphone MM310 (Microtech Gefell GmbH, Gefell, Germany). The data acquisition system was a DEWE-43 coupled with the software Dewesoft X3 (Dewesoft, Trbovlje, Slovenia). Acquisition frequency was set to 200 kHz and as a consequence the maximal detectable frequency was 78.1 kHz. Time-domain amplitude signal was converted into a frequency-domain using a fast Fourier transform (FFT) algorithm using a Blackman window with 2^{12}(=4096) points. The frequency resolution was 24.4 Hz. On each tablet at least 40 spectra were acquired.

Using the first three natural frequencies (f_1, f_2 and f_3 with $f_1 < f_2 < f_3$) obtained by impact resonance, the elastic anisotropic ratio r_{aniso} was determined using the equation of (Meynard et al., 2021a):

$$r_{aniso} = A_1 + A_2\frac{f_1}{f_2} + A_3\left(\frac{h}{D}\right)^{A_4}\left\{A_5 + expexp\left(A_6\frac{f_1}{f_3}\right) + A_7\frac{f_1}{f_2}\right\}$$

with h and D respectively the tablet thickness and diameter and $A_1 = -0.7746$, $A_2 = 0.3667$, $A_3 = 9.034 \times 10^{-4}$, $A_4 = -1.748$, $A_5 = -71.78$, $A_6 = 10.99$ and $A_7 = -68.87$.

Following the idea and methodology of (Meynard et al., 2021b), tablet viscoelastic behavior was estimated through the damping ratio related to the first tablet vibration mode. The damping ratio parameter ζ_1 was evaluated using the half-power bandwidth:

$$\zeta_1 = \frac{\Delta f}{f_1}$$

With Δf the frequency bandwidth related to the half-power amplitude $A_{max}/\sqrt{2}$ (where A_{max} is the maximum amplitude of the studied mode).

The damping ratios of all the spectra were characterized. To reduce dispersions due to the variability related to the energy excitation, the damping ratio of a product was evaluated as the mean value of the measurements made on the ten frequency spectra with the highest amplitudes of the first peak.

2.2.5. Capping quantification

Capping was quantified on a batch of ten BT tablets. A tablet with one or both of its cups coming off after manufacturing was considered as capped. An example of the considered defects can be seen in Fig. 2.

Tablets capped after manufacturing were quantified after a macroscopic examination. If no capping was observable, the tablets were then broken using the diametral compression test using the same idea as in (Akseli et al., 2013). As the use of this test made it possible to propagate an already existing crack, a tablet presenting one or both caps coming off during the diametral compression test was also considered as capped. For a batch, the capping behavior was quantified by a parameter called capping index (*CI*) corresponding to the total number of tablet presenting capping defects (after ejection and after diametral compression tests) among the total number of produced tablets (10 in the present study).

2.2.6. Predictive modelling by machine learning

To predict capping, an analysis of the influence of the properties of flat-faced tablets on BT capping behavior was made using decision trees (Breiman et al., 2017), which are a non-parametric automatic learning method. This technique was used to classify the formulations presented on the database depending on their capping behavior. We chose to separate the formulations into two classes: a) the formulations which gave non-capped tablets (i.e. $CI = 0\%$) whose class label will be "Non-capped" and b) those which led to capping defects (i.e. tablets with $CI > 0\%$) and this class will be referenced as "Capped". The dataset was subdivided into smaller groups based on binary conditions made on the data features (here, the formulations properties excluding *CI* as it is the targeted property) to subdivide the dataset until all the formulations were classified. In our decision tree, the subdivision of a group of formulations based on a threshold on a specific feature is represented by a box with two branches (two alternatives available at this node) leading thus to two child nodes. When all the formulations are classified, the terminal nodes did not split into more nodes. Thus, they represent the final outcome of a decision path obtained and will be called hereinafter leaf nodes.

At each decision node, the objective is to find the best feature which made it possible to split a group in a node in order to create purer sub-groups (i.e. sub-groups with less formulations belonging to a class miss-classified). To do so, the goodness of the split made was characterized using the Gini index $G(t)$ which quantifies, for each node t, the probability that a particular variable is wrongly classified when it is randomly chosen (i.e. the degree of impurity on the classification) and is defined as:

$$G(t) = 1 - \sum_{c\in\{Capping-free,Capped\}}[P(c|t)]^2$$

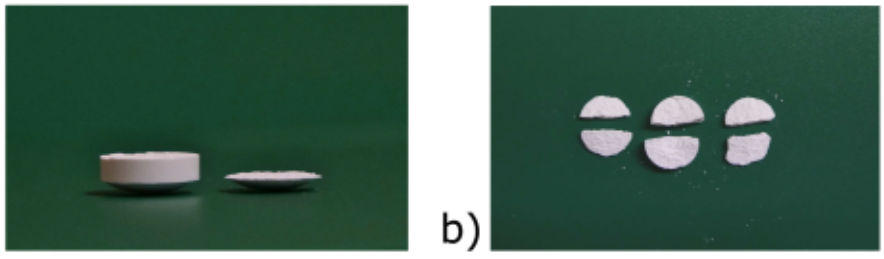

Fig. 2. Examples of capped tablets obtained a) directly out-of-the die and b) after the diametral test (both cups came off).

with $P(c|t)$ is the probability of formulations belonging to the class label c at the node t. The range of the Gini index is from 0 to 1, where 0 denotes that all the formulations in a group are in the same class and 1 represents a random distribution of the formulations among the two classes.

The threshold values at each node are calculated by the algorithm. At each decision node, the threshold X_{th} for a variable X is used to separate the set into two sub-groups A (containing all the formulations verifying $X < X_{th}$) and B (containing al the formulations such as $X > X_{th}$). X_{th} is defined as the mean value between the highest value of X in the sub-group A and the lowest value of X in the sub-group B. So the values are dependent on the dataset used.

For a given group of formulations, the feature which made it possible to divide the sub-groups as clearly as possible (the one with a highest gap between the Gini indices of the child nodes and the parent one) was used to make a decision node. The decision path was considered as complete if the leaf node was pure. When all the decision paths were obtained, using a simple Boolean logic, all the conjunctions of features leading to each class label can be identified on the obtained decision tree by studying all the combination of decision nodes leading to a class label. In this study, the Scikit-Learn Python module was used to obtain decision trees.

2.3. Methodology of the study

As explained above, our objective is to predict, using tablets made under a given manufacturing conditions (simulation of a Korsch XL 100 at 40 rpm and an axial pressure of 200 MPa), the capping behavior of tablets with a biconvex shape (BT) using the properties of flat-faced tablets made under the same manufacturing conditions. To do so, the study was performed in two parts. First, the analysis of the relationship between the properties of flat-faced tablets and the BT capping behavior was investigated on a set of formulations, referenced as training set. Then, to evaluate its accuracy, the relationship observed on the training set was tested on a new set of formulations, called the test set. For each set, the composition and the pycnometric density of each formulation studied are presented below as well as the characterizations performed.

2.3.1. Training set

Using the raw materials presented in section 1.1.1, different mixtures were performed and are presented in Table 1.

The raw powders lubricated with MgSt were called "X-l" (where X corresponds to the short name given to the raw powder used in the formulation studied – see the section above). Note that only ACP-l and TCP-20Sta had more MgSt than the others powders in order to avoid sticking issues. The other formulations were lubricated mixtures of several raw powders. The appellation was made such as it presents first the short name related to the main product in the formulation followed by the percentage of the other product. Note that the mixture "F" was made in order to mimic a platform formulation as used in the pharmaceutical field. Note also that, for each mixture having F as main component, the percentages of disintegrant and lubricant were kept fixed (5% of CNa and 1% of StMg) and the ratio between the percentage of GLac and MCC was taken as 2. The products CMan and TCP were thus used to mimic the behavior of active principles put in a platform formulation F in F-20CMan, F-40CMan and F-30TCP.

Those 18 formulations were chosen to cover a wide range of pharmaceutical products with distinct chemical structures, compositions and properties in order not to bias the study performed. For each formulation of the training set, we manufactured ten BT tablets, ten FT ones as well as five CT tablets. The capping behavior of all the formulations was quantified on BT tablets. Diametral compression tests were performed on the FT tablets. CT tablets were used for the impulse excitation tests, for the measurements of the out-of-die solid fraction and the out-of-die elastic recoveries, and for all the in-die measurements. This set of formulations was used to build the decision tree analysis to evaluate the relationship between flat-faced properties and BT capping behavior.

Table 1
Mixtures of the training set with their pycnometric density.

Formulation	Mass percent composition	ρ_{psc} (kg/m^3)
MCC-l	99% MCC + 1% MgSt	1570 ± 1
CaSul-l	99% CaSul + 1% MgSt	2294 ± 1
DCP-l	99% DCP + 1% MgSt	2306 ± 8
Ibu-l	99% Ibu + 1% MgSt	1184 ± 1
GLac-l	99% GLac + 1% MgSt	1528 ± 1
SDLac-l	99% SDLac + 1% MgSt	1541 ± 1
SDMan-l	99% SDMan + 1% MgSt	1466 ± 2
ACP-l	98% ACP + 2% MgSt	2817 ± 9
ACP60-l	99% ACP60 + 1% MgSt	2813 ± 2
GLac-30Sta	69% GLac + 30% Sta + 1% MgSt	1516 ± 1
GLac-20Par	79% GLac + 20% Par + 1% MgSt	1476 ± 1
TCP-20Sta	78% TCP + 20% Sta + 2% MgSt	2383 ± 2
SDMan-05Kol	94% SDMan + 5% Kol + 1% MgSt	1456 ± 1
CaSul-05Kol	94% CaSul + 5% Kol + 1% MgSt	2196 ± 1
F	63% GLac + 31% MCC + 5% PCNa + 1% MgSt	1554 ± 1
F-20CMan	49% GLac + 25% MCC + 20% CMan + 5% CNa + 1% MgSt	1542 ± 1
F-40CMan	36% GLac + 18% MCC + 40% CMan + 5% CNa + 1% MgSt	1528 ± 2
F-30TCP	43% GLac + 21% MCC 30% TCP + 5% CNa + 1% MgSt	1807 ± 5

2.3.2. Test set

To evaluate the accuracy of the relationship between BT capping behavior and flat-faced properties observed on the training set, different mixtures were performed for the test set. The selection of those mixtures was made in order to challenge the relationship observed on the training set. As the reasoning used for the selection of the test set was directly linked to the developed model obtained on the training set, it will be explained in details below in the results section. Using the same notations as presented previously, Table 2 shows the compositions of each mixture of the test set and their pycnometric density.

Note that, as for ACP-l of the training set, TCP-l and ACP-20Par were the only mixtures of the test set which were made with 2% of MgSt to avoid sticking issues.

For each formulation in the test set, five CT tablets were manufactured as well as ten BT ones. To evaluate the prediction given with the model developed on the training set, the in-die measurements were evaluated on the CT tablets and the capping behaviour of the BT tablets was quantified.

3. Results

3.1. Training set

The relationship between the properties of the flat-faced tablets and

Table 2
Mixtures of the test set with their pycnometric density.

Formulation	Mass percent composition	ρ_{psc} (kg/m^3)
Ala-l	99% Ala + 1% MgSt	1363 ± 1
ABenz-l	99% ABenz + 1% MgSt	1314 ± 1
PEG-l	99% PEG + 1% MgSt	1233 ± 1
TCP-l	98% TCP + 2% MgSt	2794 ± 3
Sorb-l	99% Sorb + 1% MgSt	1475 ± 1
DCSta-l	99% DCSta + 1% MgSt	1503 ± 1
Sta-l	99% Sta + 1% MgSt	1478 ± 1
ASLMP-l	99% ASLMP + 1% MgSt	1281 ± 1
GLac-10Sta	89% ACP + 10% Sta + 1% MgSt	1527 ± 1
ACP-20Par	78% ACP + 20% Par + 2% MgSt	2235 ± 1
ACP-10Sta	89% ACP + 10% Sta + 1% MgSt	2552 ± 1
ACP-15Sta	84% ACP + 15% Sta + 1% MgSt	2449 ± 1
GLac-05Kol	94% GLac + 5% Kol + 1% MgSt	1489 ± 1

the capping behavior of the BT tablets was studied on the training set. To do so, we chose to evaluate two different approaches: a) the evaluation of the capping prediction using the single parameters and indices presented in the literature and b) the development of predictive capping model using a decision tree analysis.

3.1.1. Capping prediction based on the literature

The capping behavior of BT tablets manufactured with each formulation of the training set was quantified and the results are presented in Table 3.

Eight of the 18 formulations (i.e. 44% of the database) presented capping defects with two lubricated raw products (CaSul-l and Ibu-l) and six formulations. Therefore, there were no overrepresentation of formulations leading to capped or non-capped tablets which would have led to a bias in our study. Moreover, note that F-20Man was the only formulation with a capping index between 0 and 100%. By comparing F, F-20CMan and F-40CMan, it can be observed an increase of the capping propensity of the formulation with the increase of the percentage of CMan.

In order to predict BT capping behavior, the properties of flat-faced tablets were characterized for each formulation of the training set (Fig. 3). In these graphs, formulations leading to capped tablets ($CI > 0$) are represented in dark grey where those leading to non-capped tablets ($CI = 0$) are in light grey. In order to ease the interpretation, for each property, the products were ranked in ascending order. The numerical value of each parameter can be found in the table presented in the supplementary material (Table S1).

As it can be seen in Fig. 3, the formulations studied presented also a wide range of properties of flat-faced tablets. For each tablet property, it was observed formulations that cap and formulations that led to non-capped BT tablets at both ends of the range obtained. For example, the lowest and highest values of the axial stress relaxation parameter R_{40} were obtained for formulations that led to capping whereas the second and second to last values were related to formulations giving non-capped BT tablets. Therefore, based on the study of the single parameters presented in Fig. 3, it was not possible to separate the two groups of formulations leading to capped BT tablets and non-capped ones as there was no clear threshold between those two groups. Indeed, there is no critical value in the flat-faced properties studied at which capping on BT tablets start to happen.

The absence of threshold between capped and non-capped tablets on the set of formulations challenged the predictive indicators based on a single tablet property that are presented in the literature. Indeed, for example, in the case of the residual die-wall pressure, capping is expected, based on the literature, to occur at high values of this parameter but its third highest values on the set studied were obtained for formulations leading to non-capped BT tablets.

The case of tensile strength is also interesting as it could be expected that low tensile strength should favor capping. Nevertheless, some formulations with very low tensile strength did not present capping (e.g. ACP60-l and GLac-30Sta) whereas some with a high tensile strength did (e.g. SDMan-05Kol). This demonstrates that Tabletability/compactibility studies (Tye et al., 2005), which are recommended in the literature to study compaction behavior of formulation, might not be sufficient to anticipate capping problems.

Table 3
BT capping behavior of the formulations of the training set.

Products	*CI* (%)
GLac-l; SDLac-l; SDMan-l; ACP-l; ACP60-l; DCP-l; MCC-l; GLac-30Sta; F; F-30TCP	0
F-20CMan	10
CaSul-l; Ibu-l; GLac-20Par; TCP-20Sta; SDMan-05Kol; CaSul-05Kol; F-40CMan	100

In the case of the BFI proposed by (Hiestand et al., 1977), SDLac-l is a good counterexample as its BFI of 1.40 which means that (Hiestand et al., 1977) predicted this formulation to cap (as its BFI > 0.5) whereas in fact we observed no capping defects on BT tablets ($CI = 0$). On the other hand, some of the formulations presenting capping had a low BFI (e.g. F-20Man).

The same comment can be made on the others parameters. Therefore, from a more general point of view, as no threshold was observed for each flat-faced property, counter-examples can be found for each predictive indicator based on one of those properties. Therefore, none of those properties are relevant alone to predict capping on BT tablets.

The reason for this could be that, as capping is known to be a multivariate parameter issue, its prediction should rely on indices that are a combination of various tablet parameters. Some examples of these parameters where given in the introduction. In these study, the indices of (Krycer et al., 1982) and (Sugimori et al., 1989a, 1989b) were not used for practical reason. Indeed, (Krycer et al., 1982) index required several compaction pressures for each tablet and we only manufactured tablets at 200 MPa for this study. In the case of (Sugimori et al., 1989a, 1989b) index, experiments on flat-faced tablets with a thickness of about 8 mm were required. As the comparability between those very thick tablets and 2-mm thick tablets (geometry used in this study) could be questionable, we chose not to evaluate this parameter.

Using the properties characterized on the database, we chose to evaluate two of those predictive indices:

- Based on the study of (Nakamura et al., 2012), we estimated the parameter I_N as:

$$I_N = E_{p,\iota} R_{40}$$

The plastic energy was normalized per its volume (Wünsch et al., 2021) and the axial stress relaxation was approximated with the tablet relaxation during the dwell-time of the manufacturing cycle. According to Nakamura et al., low values of I_N should be related to high propensity to cap.

- Based on the study of (Akseli et al., 2013), we characterized this parameter as:

$$I_A = \frac{P_\gamma E_{O,H}}{\sigma_T}$$

Under the assumption that the in-die and the out-of-die Heckel parameters are strongly correlated (Vreeman and Sun, 2021), we chose to use the in-die P_γ that was characterized in this study instead of the out-of-die parameter used in (Akseli et al., 2013). The tensile strength measured on FT tablets was used instead of the one obtained on CT tablets as it is a better estimation of tablet strength (Mazel et al., 2016). Moreover, note that in (Akseli et al., 2013), a number 40 was put into the equation to normalize the index value. However, due to the modifications that we made, we will only focus on the curve tendency and not on the proper value of this index. High values of I_A are expected to be related to high tendency to cap.

Fig. 4 shows the estimations of the two predictive capping indices studied for all the formulations of the training set.

Results are similar to those presented in Fig. 3 for predictors based on single tablet property. Formulations leading to capped BT tablets were found for high values and low values of both indicators. Therefore, even if capping is expected for low values of I_N and high values of I_A, examples can be found on both sides of the graph for both indicators in the training set such as DCP-l (low I_N and non-capped BT tablets) and TCP-

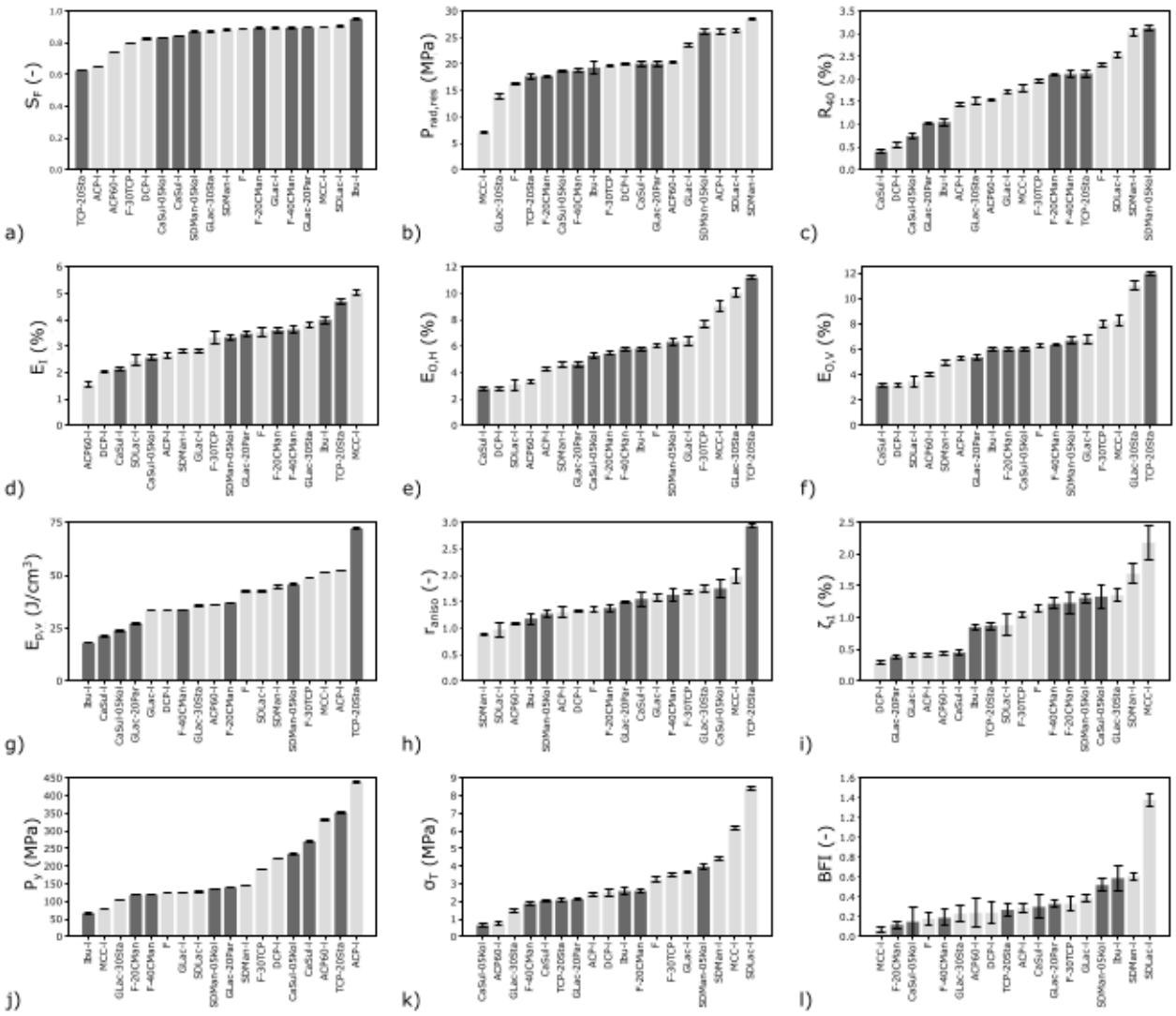

Fig. 3. Results on flat-faced tablets in terms of a) solid fraction, b) residual die-wall pressure, c) axial stress relaxation parameter, d) in-die elastic recovery, e) out-of-die height elastic recovery, f) out-of-die volume elastic recovery, g) plastic energy per volume, h) elastic anisotropic ratio, i) damping ratio, j) Heckel parameter, k) tensile strength and l) BFI. Formulations leading to capped tablets (CI > 0) are represented in dark grey where those leading to non-capped tablets (CI = 0) are in light grey.

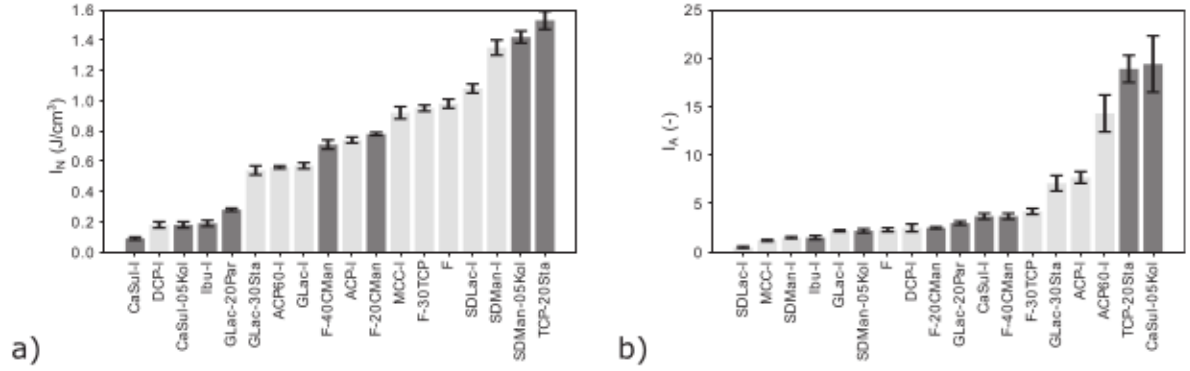

Fig. 4. Estimation of the predictive capping indices: a) Nakamura index and b) Akseli index. Results in ascending order with in dark grey the formulations leading to BT capped tablets and in light grey those giving non-capped ones.

20Sta (high I_N and capped BT tablets) for I_N and ACP60-l (high I_A and non-capped BT tablets) and Ibu-l (low I_A and capped BT tablets) for I_A. Therefore, the predictive indices (as well as the predictors based on single tablet property) presented in the literature did not make it possible to discriminate capping behavior of the formulations studied.

The fact that the predictive indicators of the literature did not make it possible to predict capping could come from the fact that the failure of a tablet by capping can occur for several distinct combinations of

properties, i.e. different kinds of capping situations might exist. Therefore, an indicator might not be sufficient to predict capping for each situation causing the defect. To evaluate the hypothesis of different paths leading to capping, we chose to analyze the training set using a decision tree classification.

3.1.2. Development of a predictive model using a machine learning tool

Another possibility to predict the capping behavior of BT tablets using the properties of flat-faced tablets is to study the training set using machine learning tools. In recent years, machine learning was increasingly used in the pharmaceutical field to predict tablet properties (Paul et al., 2021; Paul and Sun, 2017; Plumb et al., 2005). To the authors knowledge, (Paul et al., 2021) is the only article with a topic similar to the one of the present article as they investigated for bevel-edged tablets the relationship between their properties (tablet strength, Heckel parameter, …) and their capping behaviour using statistical analyses. However, they characterized indirectly the capping behaviour of their tablets using the anisotropic ratio based on Young moduli presented by (Akseli et al., 2013) and they did not validate through mechanical tests that they actually observed capping defects. It is not clear from the article if capped tablet were effectively obtained. Moreover, several different machine learning tools are presented and give contradictory results. Results are thus difficult to fully interpret.

In order to study the key tablet properties impacting capping, we chose to make a decision tree analysis on the training set. We chose this method as it could make it possible to identify different combinations of properties leading to capping. A model based on the database obtained was developed using a decision tree analysis and is presented in Fig. 5.

Using a decision tree analysis, it was possible to classify all the formulations of the training set (Fig. 5). Thus, this model indicated, for the dataset studied, a relationship between BT capping behaviour and flat-faced tablet properties of the training set. Note that, for each decision path obtained, they were lubricated pure products as well as mixtures mimicking industrial formulations (Table 4). Therefore, it seemed that the model did not artificially segregate the products in terms of compositions or chemical structures (which would have been a model bias) but really in terms of their properties.

Three parameters were required in this model to classify the BT capping behaviour of the training set using the flat-faced tablet properties: the plastic energy per volume $E_{p,v}$, the in-die elastic recovery E_I and the residual die-wall pressure $P_{rad,res}$. This model presented two decision paths leading to the appearance of capping defects: a) the formulations with low plastic energy per volume and b) those with high $E_{p,v}$, E_I and $P_{rad,res}$. It is worth noting that the threshold values for each parameter might depend on the manufacturing conditions used (kept constant in the present study) and thus should not be taken as absolute values.

Table 4
Classification of the formulations on the training set. The decision path is the set of features and their values required to reach the leaf node studied.

Class	Decision path	Formulations
Non-capped	($E_{p,v}$, E_I) →(No, Yes)	GLac-l; SDLac-l; CMan-l; ACP-l; ACP60-l; DCP-l; F-30TCP
	($E_{p,v}$, E_I, $P_{rad,res}$) →(No, No, Yes)	MCC-l; GLac-30Sta; F
Capped	($E_{p,v}$) →(Yes)	CaSul-l; Ibu-l; GLac-20Par; CaSul-05Kol
	($E_{p,v}$, E_I, $P_{rad,res}$) →(No, No, No)	TCP-20Par; SDMan-05Kol; F-20CMan; F-40CMan

The effects of the elastic recovery and the residual-die wall pressure and their entanglement had been already presented by (Hiestand et al., 1977; Mazel et al., 2015). Indeed, as explained above, during the unloading phase when the contact between the punches and the tablet is lost, there is a development of a shear stress between the land and the cup. Increasing the elastic recovery induces more stress on the region where the shear stress appears. The increase of the residual die-wall pressure leads also to an increase of the shear stress distribution. This combination of parameters therefore seems logical considering the mechanism.

However, what this model indicates is that the combination of $P_{rad,res}$ and E_I did not make it possible to predict capping for all formulations and another capping situation corresponds to low $E_{p,v}$. For those products, for whatever combinations of $P_{rad,res}$ and E_I, all the formulations studied were capped. Therefore, for formulations with low $E_{p,v}$, capping occurred for another reason. Several authors have already shown the importance of this parameter through the study of elastic–plastic energetic diagram on the inter-particulate cohesion (de Blaey and Polderman, 1970; Garekani et al., 2001; Nakamura et al., 2012; Ragnarsson and Sjögren, 1985). Nevertheless, the interpretation of $E_{p,v}$ remains unclear as this parameter includes the energy related to plastic deformations including all the energies consumed by the process (such as plastic flow, particulate fragmentation, adhesion and re-arrangement) or lost during the process such as by friction. However, depending on the product, the amount of energy necessary for each phenomenon could vary (De Boer et al., 1978).

Note that, besides from $E_{p,v}$, there is another parameter used in the pharmaceutical field usually used to evaluate the plastic behaviour of

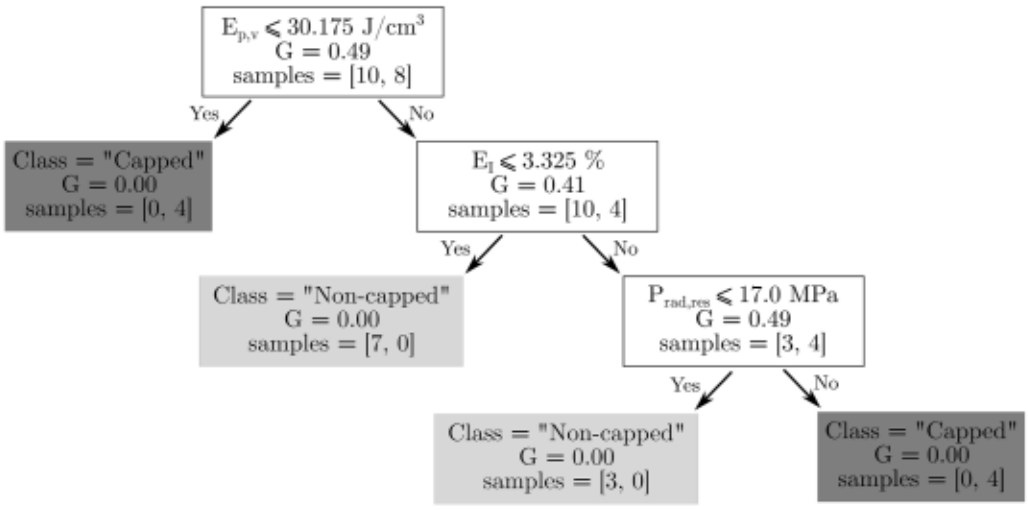

Fig. 5. Decision tree obtained with the study of the database. At each node, the parameter samples = [X, Y] in the graph gave the X formulations which gave experimentally non-capped tablets and the Y ones giving capped tablets.

compressed formulations: the Heckel parameter. It is often used to describe the formulation ductile behaviour through its yield pressure even if this use could be questionable for pharmaceutical mixtures (Sonnergaard, 1999). Even if the interpretation of P_y is questionable, it can be considered as a correct indicator of the resistance of a powder to plastic deformations (Vreeman and Sun, 2021). To test the relationship between $E_{p,v}$ and P_y, a correlation analysis between the two parameters evaluated on the training set was performed and gave a coefficient of 0.34. This low value showed that there is almost no relationship between $E_{p,v}$ and P_y. Thus, those two parameters did not describe the same phenomena occurring during compaction and must be used carefully.

One interesting point of this model is that it involves none of the variables related to tablet strength such as the tensile strength or the BFI. This can seem surprizing. Nevertheless, as the rational of $E_{p,v}$ is not fully understood, it is possible that it might in fact reflect some aspects of the tablet cohesion acquisition during manufacturing. However, if this relation exists, it is not straightforward considering the data as there is, in the data, no correlation between $E_{p,v}$ and σ_T (correlation coefficient of 0.31).

Another interesting point of the obtained model is that all the properties presented were in-die ones. As capping is a defect which appears in-die during the unloading phase (Hiestand et al., 1977; Mazel et al., 2015), this might seem logical. If this model proved to be largely applicable, it will of course be of interest from an industrial point of view, as all the properties can be tested by the manufacturing of a very limited number of tablets (it can even be evaluated using one tablet).

The developed model obtained using the decision tree algorithm was the only method that made it possible to classify the capping behaviour of the formulations in the training set based on their flat-faced tablet properties. In order to test the developed predictive model, a set of formulations was chosen in order to investigate the validity of this model.

3.2. Test set

The test set was used to evaluate the accuracy of the prediction of the model obtained using a decision tree analysis on the 18 formulations of the training set. As presented above, this model depends on three parameters: $E_{p,v}$, E_l and $P_{rad,res}$. Therefore, we tried to select, for the test set, formulations which could challenge the model obtained and which were different from the ones used in the training set. For example, we added formulations by changing the "drug" load and the components of mixtures used on the training set to obtain cases close to the conditions presented on the decision path of the developed model. The 13 formulations selected for the test set are presented in section 1.3.2. Note that, as the developed model to test required only the in-die properties, we only performed the in-die measurements (which required to manufacture only five CT tablets and characterize their mass and density). The estimation of capping with this model was thus convenient as the characterizations necessary were quick and easy. Moreover, it made it possible to test powders that would have been difficult to include in the first set because some properties might have been difficult to characterize (e.g. BFI for very weak tablets).

3.2.1. Verification of the accuracy of the developed model

Table 5 shows the prediction of the class for the formulations on the test set based on the developed model. The numerical values of the properties characterized on the formulations of the test set leading to the decisions paths presented on Table 5 are shown in the supplementary material (Table S2).

To evaluate the accuracy of the capping prediction, BT tablets were manufactured for each formulation of the test set and their capping index *CI* were characterized. The comparison between the estimated classes and the experiments are shown in Fig. 6.

As it can be seen in Fig. 6, the capping behavior of 11 out of the 13 formulations in the test was well estimated, which corresponds to a

Table 5
Prediction of the capping behavior on BT tablets of the formulations on the training set.

Decision path	Formulations	Predicted class
($E_{p,v}$, E_l) →(No, Yes)	Sorb-l; GLac-10Sta; ACP-10Sta; GLac-05Kol	Non-capped
($E_{p,v}$, E_l, $P_{rad,res}$) →(No, No, Yes)	Sta-l; DCSta-l; ASLMP-l	Non-capped
($E_{p,v}$) →(Yes)	Ala-l; ABenz-l; PEG-l	Capped
($E_{p,v}$, E_l, $P_{rad,res}$) →(No, No, No)	TCP-l; ACP-15Sta; ACP-20Par	Capped

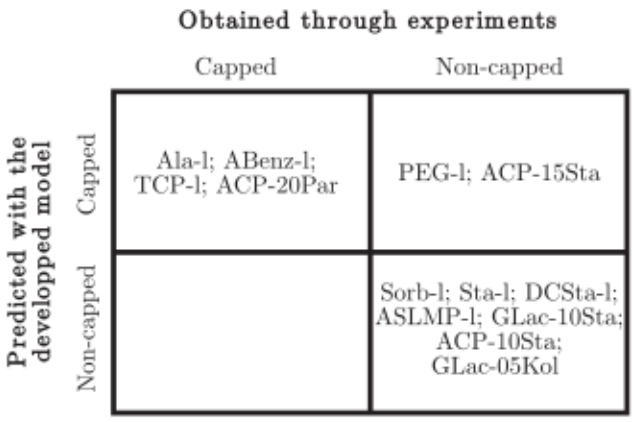

Fig. 6. Comparison between the experiments and the results of the classification model.

classification accuracy of about 85% for the developed predictive model. It is worth noting that 29 of the 31 formulations (from the training and the test sets) were classified in the class in line with the characterizations made on BT tablets and we only found 2 misclassified mixtures: PEG-l and Em-15Sta. Based on its high classification accuracy rate, the developed model seemed to be a good predictive estimator of the capping behavior of BT tablets using properties measured on flat-faced tablets.

The two misclassified products belonged to the non-capped class based on the characterizations performed on the BT tablets and the model prediction wrongly put them in the capped class. Note that we found no product that was found capped experimentally and classified as non-capped by the model. This means that all the formulations predicted as non-capped, were correctly predicted which interesting from a risk analysis perspective.

However, the presence of 2 misclassified products showed that all the combinations of properties leading to capping were not well described in the developed model. In order to understand the model weaknesses, these two misclassified formulations were studied in details.

3.2.2. Study of the misclassified formulations

Two of the test set were misclassified: PEG-l and ACP-15Sta (see Table 5). To better understand their misclassification, a full characterization on flat-faced tablets of those two products was performed. Table 6 shows the results and, for each property, the rank of the formulation compared to the properties of the training set was given by increasing order in parenthesis, with 1 and 20 corresponding respectively to the lowest and highest values.

Compared to the other products, PEG-l presented properties to the high or low end of the database features such as a rather non-existent axial stress relaxation, an important viscoelastic behaviour (highest damping ratio) and the lowest residual die-wall pressure. As it can be seen with its low BFI, it was the studied product whose value of tensile strength was the least sensible to the presence of defects in its

Table 6
Properties of the flat-faced tablets for the two misclassified products (in parenthesis order of the product by increasing order with 1 and 20 corresponding respectively to the lowest and highest values).

Product	S_F (-)	$P_{rad,res}$ (MPa)	R_{40} (%)	E_l (%)	$E_{O,H}$ (%)	$E_{O,V}$ (%)	$E_{p,v}$ (J/cm^3)	r_{Aniso} (-)	ζ_1 (-)	P_y (MPa)	σ_T (MPa)	*BFI* (-)
PEG-l	0.927 ± 0.002 (19th)	2.9 ± 0.5 (1st)	0.01 ± 0.07 (1st)	4.54 ± 0.17 (18th)	11.42 ± 0.17 (20th)	9.84 ± 0.16 (18th)	18.71 ± 0.16 (2nd)	0.84 ± 0.03 (1st)	3.23 ± 0.29 (20th)	29.5 ± 0.6 (1st)	1.38 ± 0.03 (3rd)	0.06 ± 0.03 (1st)
ACP-15Sta	0.691 ± 0.002 (3rd)	19.4 ± 0.2 (10th)	1.76 ± 0.02 (11th)	3.66 ± 0.06 (15th)	8.13 ± 0.19 (16th)	9.48 ± 0.20 (17th)	49.95 ± 0.42 (17th)	1.38 ± 0.05 (11th)	0.93 ± 0.05 (10th)	287.8 ± 0.7 (17th)	2.03 ± 0.03 (7th)	0.18 ± 0.04 (6th)

microstructure as it was able to release stress through ductile deformations. Its misclassification on the decision path "($E_{p,v}$) (Yes)" underlines the problematic interpretation of $E_{p,v}$ as explained previously. To illustrate this, we can compare PEG-l ($E_{p,v}$ of about 18 J/cm^3) and CaSul-l ($E_{p,v}$ of about 20 J/cm^3), which are both classified as capped by the tree based on their low $E_{p,v}$. The plastic deformations involved in the manufacturing of both of those products can be reasonably considered different. Indeed, PEG-l is a polymer with a very low resistance to plastic deformations (P_y = 29.5 MPa) whereas CaSul-l is a crystalline product which is resistant to plastic deformations (P_y = 269.4 MPa). As such, even if $E_{p,v}$ is close for both products, it might in fact cover very different microscopic phenomena related to plasticity which might be a reason for the misclassification of PEG-l. Nevertheless, as it is a quite unique product in our dataset, it is difficult to go further on the understanding of this misclassification.

The case of ACP-15Sta (the other misclassified product) was proposed, considering the results of ACP-l in the training set. As presented above (Table 4), ACP-l was classified as non-capped because it had a large $E_{p,v}$, but a small E_l. It also had a high $P_{rad,res}$ (Fig. 3), way above the threshold of the model (even if it was not used for its classification because this parameter is only considered in the tree for high $E_{p,v}$ and high E_l). Our idea was to try to make a mixture using ACP that could be predicted as capped. To do so, we mixed it with Sta, which is known to be an elastic product, to increase the in-die elastic recovery. The results are presented in Fig. 7.

In a first try, we used 10% (ACP-10Sta). As expected, it increased E_l but not enough to overpass the threshold related to this parameter (with an $E_{p,v}$ still way above its threshold). It also reduced the value of $P_{rad,res}$ but without going below the threshold for this variable. The use of 15% Sta (ACP-15Sta) made it possible to overpass the threshold in E_l and to keep a value of $P_{rad,res}$ above the limit given by the tree, which gave thus a classification as capped for this formulation. Nevertheless, experiments on BT tablets showed no sign of capping for ACP-15Sta. Therefore, by playing with the drug load of mixtures with properties close to the decision nodes, it was possible to challenge the transitions expressed by those nodes. The fact that ACP-15Sta was misclassified showed thus that the transition zones (combinations of properties close the those of the decision nodes) might still require some investigations in order to predict correctly capping in these zones.

4. Conclusion

This work aimed to study how it could be possible to predict the capping behavior of biconvex tablets made under specific manufacturing conditions (Korsh XL100, 200 MPa and made with Euro-B 11.28R11 punches) using the properties of defect-free flat-faced tablets made under the same conditions. The investigation of twelve properties (proposed by the literature) impacting capping was made on 18 products, differing in chemical structures, compositions and properties.

First, it was found that the use of single parameters failed to predict correctly the behavior of the studied formulations. For example, tensile strength was not found to be relevant as we found capping situations on formulation with both high and low tensile strength. This result shows that tabletability/compactibility studies might not be enough for capping prediction. As capping might be caused by multiple factors, predictive indices (calculated from a combination of single parameters) were also tested but without success.

Those results seemed to indicate that several capping situations might exist. Considering this idea, a machine leaning analysis based on a decision tree classification was used on the database in order to predict capping. Thanks to this analysis, it was possible to find a tree predicting the capping behavior of the 18 formulations. This tree was then tested on 13 other formulations and gave a correct capping prediction for 11 of them. Note that the evaluation of non-capped tablets was always accurate on the set studied, showing that the safe combinations properties leading to non-capped tablets can be well predicted with this model.

The classification tree found used only three in-die parameters: the plastic energy per volume, the in-die elastic recovery and the residual die-wall pressure. It is interesting to note that strength parameters like tensile strength or BFI were not present in the model, which challenges the classical view of capping. Nevertheless, a complete understanding of the plastic energy per volume is still missing in order to fully understand the logic of the tree obtained. This will be developed in future works.

The estimation of capping with the developed method (29 out of 31, i.e. 93.5%) is encouraging and indicates that this approach is reliable. Of

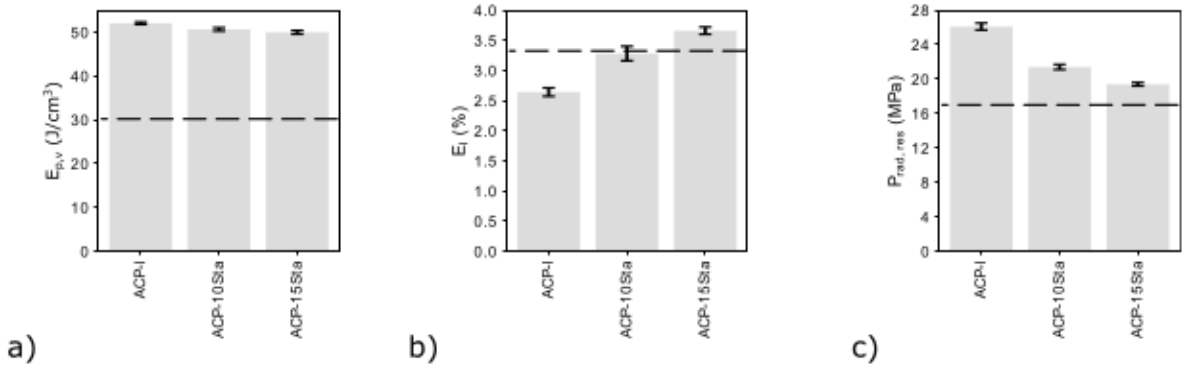

Fig. 7. Comparison of the parameters used in the develop model with the values of decision nodes (dashed lines) for ACP-10Sta and ACP-15Sta.

course, more work is necessary to complete this study as, for example, the manufacturing conditions were kept constant (compaction condition, speed and the tablet shape used to evaluate capping) in the present study. It is worth noting that the threshold values found in the tree are only indicative of the conditions used in the present study and are dependent on the values of the dataset. They should thus not be taken as absolute values. Nevertheless, as a large number of different kinds of formulations were studied, the classification order should be applicable to other situations. This kind of approach might thus be of practical use in the future in the context of a risk assessment analyses for capping occurrence.

CRediT authorship contribution statement

J. Meynard: Methodology, Investigation, Conceptualization, Writing – original draft. **F. Amado-Becker:** Conceptualization, Writing – review & editing. **P. Tchoreloff:** Writing – review & editing. **V. Mazel:** Methodology, Conceptualization, Writing – review & editing.

Declaration of Competing Interest

The authors declare that they have no known competing financial interests or personal relationships that could have appeared to influence the work reported in this paper.

Data availability

Data will be made available on request.

Appendix A. Supplementary data

Supplementary data to this article can be found online at https://doi.org/10.1016/j.ijpharm.2022.121949.

References

Akseli, I., Ladyzhynsky, N., Katz, J., He, X., 2013. Development of predictive tools to assess capping tendency of tablet formulations. Powder Technol., Special Issue: Pharmaceutical Powders 236, 139–148.

Alderborn, G., 2001. Tablets and compaction, in: Aulton's Pharmaceutics: The Design and Manufacture of Medicines. Churchill Livingstone, London.

Armstrong, N.A., Haines-Nutt, R.F., 1974. Elastic recovery and surface area changes in compacted powder systems. Powder Technol. 9, 287–290. https://doi.org/10.1016/0032-5910(74)80054-9.

Breiman, L., Friedman, J.H., Olshen, R.A., Stone, C.J., 2017. Classification And Regression Trees. Routledge, New York. https://doi.org/10.1201/9781315139470.

de Blaey, C.J., Polderman, J., 1970. Compression of pharmaceuticals. I. The quantitative interpretation of force-displacement curves. Pharm. Weekbl. 105, 241–250.

De Boer, A.H., Bolhuis, G.K., Lerk, C.F., 1978. Bonding characteristics by scanning electron microscopy of powders mixed with magnesium stearate. Powder Technol. 20, 75–82. https://doi.org/10.1016/0032-5910(78)80011-4.

Garekani, H.A., Ford, J.L., Rubinstein, M.H., Rajabi-Siahboomi, A.R., 2001. Effect of Compression Force, Compression Speed, and Particle Size on the Compression Properties of Paracetamol. Drug Dev Ind Pharm 27, 935–942. https://doi.org/10.1081/DDC-100107674.

Haware, R.V., Tho, I., Bauer-Brandl, A., 2010. Evaluation of a rapid approximation method for the elastic recovery of tablets. Powder Technol. 202, 71–77. https://doi.org/10.1016/j.powtec.2010.04.012.

Heckel, R.W., 1961a. Density-pressure relationships in powder compaction. Trans Met. Soc AIME 221, 671–675.

Heckel, R.W., 1961b. An analysis of powder compaction phenomena. Trans Met. Soc AIME 221, 1001–1008.

Hiestand, E.N., Wells, J.E., Peot, C.B., Ochs, J.F., 1977. Physical Processes of Tableting. J. Pharm. Sci. 66, 510–519. https://doi.org/10.1002/jps.2600660413.

Hirschberg, C., Paul, S., Rantanen, J., Sun, C.C., 2020. A material-saving and robust approach for obtaining accurate out-of-die powder compressibility. Powder Technol. 361, 903–909. https://doi.org/10.1016/j.powtec.2019.11.004.

Krycer, I., Pope, D.G., Hersey, J.A., 1982. The prediction of paracetamol capping tendencies. J. Pharm. Pharmacol. 34, 802–804. https://doi.org/10.1111/j.2042-7158.1982.tb06229.x.

Maganti, L., Çelik, M., 1993. Compaction studies on pellets I. Uncoated pellets. Int. J. Pharm. 95, 29–42. https://doi.org/10.1016/0378-5173(93)90387-U.

Mazel, V., Busignies, V., Diarra, H., Tchoreloff, P., 2013. On the Links Between Elastic Constants and Effective Elastic Behavior of Pharmaceutical Compacts: Importance of Poisson's Ratio and Use of Bulk Modulus. J. Pharm. Sci. 102, 4009–4014. https://doi.org/10.1002/jps.23710.

Mazel, V., Diarra, H., Busignies, V., Tchoreloff, P., 2015. Evolution of the Die-Wall Pressure during the Compression of Biconvex Tablets: Experimental Results and Comparison with FEM Simulation. J. Pharm. Sci. 104, 4339–4344. https://doi.org/10.1002/jps.24682.

Mazel, V., Guerard, S., Croquelois, B., Kopp, J.B., Girardot, J., Diarra, H., Busignies, V., Tchoreloff, P., 2016. Reevaluation of the diametral compression test for tablets using the flattened disc geometry. Int. J. Pharm. 513, 669–677. https://doi.org/10.1016/j.ijpharm.2016.09.088.

Mazel, V., Tchoreloff, P., 2020. Applicability of impulse excitation technique as a tool to characterize the elastic properties of pharmaceutical tablets: Experimental and numerical study. Int J Pharm 590, 119892. https://doi.org/10.1016/j.ijpharm.2020.119892.

Meynard, J., Amado-Becker, F., Tchoreloff, P., Mazel, V., 2021. Use of impulse excitation technique for the characterization of the elastic anisotropy of pharmaceutical tablets. Int. J. Pharm. 605, 120797 https://doi.org/10.1016/j.ijpharm.2021.120797.

Meynard, J., Amado-Becker, F., Tchoreloff, P., Mazel, V., 2022. Characterization of the viscoelasticity of pharmaceutical tablets using impulse excitation technique. Int. J. Pharm. 613, 121410.

Nakamura, H., Sugino, Y., Watano, S., 2012. In-Die Evaluation of Capping Tendency of Pharmaceutical Tablets Using Force-Displacement Curve and Stress Relaxation Parameter. Chem Pharm Bull Tokyo 60, 772–777. https://doi.org/10.1248/cpb.60.772.

Nyström, C., Malmqvist, K., Mazur, J., Alex, W., Hölzer, A., 1978. Measurement of axial and radial tensile strength of tablets and their relation to capping. Acta Pharm. Suec. 15, 226–232.

Okor, R.S., Eichie, F.E., Ngwa, C.N., 1998. Correlation Between Tablet Mechanical Strength and Brittle Fracture Tendency. Pharm. Pharmacol. Commun. 4, 511–513. https://doi.org/10.1111/j.2042-7158.1998.tb00665.x.

Paul, S., Baranwal, Y., Tseng, Y.-C., 2021. An insight into predictive parameters of tablet capping by machine learning and multivariate tools. Int. J. Pharm. 599, 120439 https://doi.org/10.1016/j.ijpharm.2021.120439.

Paul, S., Sun, C.C., 2017. Gaining insight into tablet capping tendency from compaction simulation. Int. J. Pharm. 524, 111–120. https://doi.org/10.1016/j.ijpharm.2017.03.073.

Picker, K.M., 2001. Time Dependence of Elastic Recovery for Characterization of Tableting Materials. Pharm. Dev. Technol. 6, 61–70. https://doi.org/10.1081/PDT-100000014.

Plumb, A.P., Rowe, R.C., York, P., Brown, M., 2005. Optimisation of the predictive ability of artificial neural network (ANN) models: A comparison of three ANN programs and four classes of training algorithm. Eur. J. Pharm. Sci. 25, 395–405. https://doi.org/10.1016/j.ejps.2005.04.010.

Ragnarsson, G., Sjögren, J., 1985. Force-displacement measurements in tableting. J Pharm Pharmacol 37, 145–150. https://doi.org/10.1111/j.2042-7158.1985.tb05029.x.

Ritter, A., Sucker, H.B., 1980. Studies of variables that affect tablet capping. J. Pharm. Technol. 3, 24–33.

Sonnergaard, J.M., 1999. A critical evaluation of the Heckel equation. Int. J. Pharm. 193, 63–71. https://doi.org/10.1016/S0378-5173(99)00319-1.

Sugimori, K., Mori, S., Kawashima, Y., 1989a. Characterization of die wall pressure to predict capping of flat- or convex-faced drug tablets of various sizes. Powder Technol 58, 259–264. https://doi.org/10.1016/0032-5910(89)80052-X.

Sugimori, K., Mori, S., Kawashima, Y., 1989b. Introduction of New Index for the Prediction of Capping Tendency of Tablets. Chem Pharm Bull Tokyo 37, 458–462. https://doi.org/10.1248/cpb.37.458.

Tye, C.K., Sun, C. (Calvin), Amidon, G.E., 2005. Evaluation of the effects of tableting speed on the relationships between compaction pressure, tablet tensile strength, and tablet solid fraction. J. Pharm. Sci. 94, 465–472. https://doi.org/10.1002/jps.20262.

Vreeman, G., Sun, C.C., 2021. Mean yield pressure from the in-die Heckel analysis is a reliable plasticity parameter. Int J Pharm X 3, 100094. https://doi.org/10.1016/j.ijpx.2021.100094.

Wood, J.R., 1906. Tablet Manufacture: Its History. Pharmacy and Practice, JB Lippincott Company.

Wu, C.-Y., Hancock, B.C., Mills, A., Bentham, A.C., Best, S.M., Elliott, J.A., 2008. Numerical and experimental investigation of capping mechanisms during pharmaceutical tablet compaction. Powder Technol. Particulate Processes in the Pharmaceutical Industry 181, 121–129. https://doi.org/10.1016/j.powtec.2006.12.017.

Wünsch, I., Michel, S., Finke, J.H., John, E., Juhnke, M., Kwade, A., 2021. How can single particle compression and nanoindentation contribute to the understanding of pharmaceutical powder compression? Eur. J. Pharm. Biopharm. 165, 203–218. https://doi.org/10.1016/j.ejpb.2021.05.009.

Yohannes, B., Gonzalez, M., Abebe, A., Sprockel, O., Nikfar, F., Kang, S., Cuitino, A.M., 2015. The role of fine particles on compaction and tensile strength of pharmaceutical powders. Powder Technol. 274, 372–378. https://doi.org/10.1016/j.powtec.2015.01.035.